Advances in Clinical Radiology 1 (2019) 109–118
ADVANCES IN CLINICAL RADIOLOGY

Quantitative Computed Tomographic Evaluation of Lung Nodules

Jeffrey B. Alpert, MD
Department of Radiology, Thoracic Imaging, NYU Langone Health, 660 First Avenue, 3rd Floor, New York, NY 10016, USA

KEYWORDS
• Quantitative CT • Lung nodule • Subsolid lung nodule • Nodule volumetry • First-order statistics • Histogram • Texture analysis

KEY POINTS
- Quantitative computed tomographic (CT) evaluation of lung nodules has achieved significant progress through the continued evolution of technical imaging and data-processing capabilities, with an ever-growing body of literature using first- and second-order statistical evaluation.
- Quantitative CT has shown considerable promise in assessment of indeterminate subsolid lung nodules, with the goal of accurately diagnosing lung adenocarcinoma subtypes based on quantitative imaging features. Such success could significantly impact patient management.
- Standardized definitions and nomenclature used to describe quantitative CT are necessary.
- Standardized research methodology and data-processing techniques can strengthen the growing body of literature and make quantitative CT imaging more accessible to practicing radiologists.

INTRODUCTION

Traditionally, and even today, most image interpretation performed by radiologists is subjective: visual inspection of an image by an experienced reader. Although quantitative measurements like size and density can be obtained, this information is acquired in response to an initial visual assessment as the radiologist considers a diagnosis and the potential likelihood for harm. Even among the most experienced radiologists, there exists an element of subjectivity, and therefore, variability. As clinicians' reliance on imaging continues to grow, and with it the expectation of accurate radiologic diagnosis, it may be wise to consider that with computed tomography (CT), for example, there is a great deal of valuable imaging data that subjective visual assessment fails to capture. Quantitative CT imaging attempts to maximize information from unrecognized or underutilized data that are already routinely acquired during imaging, using novel software to process data at the level of the voxel.

As can be seen in the literature, investigators have embraced the potential for quantitative CT imaging. However, on the subject of the indeterminate pulmonary nodule, a synergistic union can be found: significant advancement in technical imaging and data-processing capabilities, applied to a clinically relevant topic, which continuously seeks improved diagnosis and prognostication through imaging. Quantitative CT has shown particular promise in the evaluation of subsolid lung nodules, comprising ground-glass or part-solid visual attenuation, because they may histopathologically represent lesions on a spectrum of adenocarcinoma diagnoses. The ability of quantitative CT imaging to aid in preoperative or even nonoperative diagnosis of these adenocarcinoma subtypes is becoming more fully realized, with immense potential

There are no commercial or financial conflicts of interest to disclose. No funding was provided for this work.
E-mail address: jeffrey.alpert@nyulangone.org

https://doi.org/10.1016/j.yacr.2019.04.004
2589-8744/19/

to impact clinical management of patients with previously indeterminate lung nodules. This intersection of progress in the technical and clinical realms presents a unique opportunity to generate a significant positive impact on clinical care.

Discussion of quantitative CT evaluation of lung nodules encompasses a spectrum of complexity: nodule size can be measured by diameter, cross-sectional area, or volume. By determining nodule attenuation, mass can be determined. Further investigation can be performed using first-order statistics, most commonly using histogram evaluation of nodule attenuation at the level of the voxel, as well as second-order statistics, often referred to as texture analysis. This article serves as an introduction to quantitative CT evaluation of lung nodules, focused on descriptive explanations of prevalent radiomics features, current literature, and ongoing challenges.

NODULE DIAMETER, VOLUME, AND MASS

Quantitative CT assessment of lung nodules encompasses a wide spectrum of nodule measurements and features. Unidimensional or bidimensional nodule diameter can be determined with the use of manually placed electronic calipers; this remains the most widely accepted method of lung nodule measurement, although limitations posed by interobserver and intraobserver variability are well known [1,2]. An important study by Revel and colleagues [2] reported an interreader variability of nodule diameter of 1.73 mm (or approximately 20%) for a group of lung nodules with a mean diameter of 8.5 mm. It is worthwhile to note that mathematically a variation of 20% in diameter is comparable to a variation of nearly 100% in volume [3]. Current management guidelines from the Fleischner Society for incidentally detected lung nodules are based on nodule size determined by an average of bidimensional measurements [4]. However, nodule volume thresholds are now incorporated into the management guidelines for both solid and subsolid lung nodules, with a small lung nodule measuring up to 6 mm corresponding to an estimated volumetric measurement of up to 100 mm^3.

Although methods to determine lung nodule volume have yet to become fully streamlined into the typical radiology reading room, nodule volumetry has been shown to be a more sensitive indicator of lung nodule growth: volumetric nodule measurement does not assume a perfectly spherical nodule shape, as an accurate bidimensional measurement would require, and serial volumetric measurement allows determination of volumetric doubling time, thought to more reliably reflect nodule growth (Fig. 1) [3]. Successful implementation of lung nodule volumetry is perhaps best illustrated by lung cancer screening trials, such as the European NELSON (Nederlands-Leuvens Longkanker Screenings Onderzoek) screening trial, which assessed noncalcified lung nodules by volume and volume-doubling time (VDT). In this large-scale investigation, a nodule volume of 100 mm^3 or smaller correlated with a maximum transverse nodule diameter less than 5 mm and was thought unlikely to reflect malignancy, whereas an intermediate nodule measuring 100 to 300 mm^3 correlated with a diameter of approximately 5 to 10 mm and was further assessed by VDT to predict the likelihood of developing lung cancer within 2 years of the initial CT scan, with growth determined as an increase in volume of 25% or more [5,6]. A high-probability nodule measuring 300 mm^3 or more correlated with nodule diameter of 10 mm or larger and was immediately investigated further. Notably, these volumetry-based nodule protocols resulted in equal or higher sensitivity and specificity for diagnosis of malignancy when compared with the well-established American College of Chest Physician nodule management protocol [5,7,8]. In a related study by the research group, an optimized VDT cutoff was determined for rapidly growing solid nodules detected in the lung cancer screening program [9]. All malignant fast-growing nodules in the group had a VDT of less than or equal to 232 days; applying this cutoff resulted in a reduction in false-positive pulmonary referrals of up to 33%. In a separate study by Mehta and colleagues [10], lung nodule volume was incorporated into a malignancy prediction model for incidental lung nodules detected on CT, resulting in significant improvement in performance of the prediction model by roughly 20%.

Lung nodule volumetry has proven to be a reliable method to assess nodule size and growth. Semiautomated software has been shown to provide highly reproducible volumetric results, better than the reported reproducibility of simple linear measurements or even manually derived nodule volumes [11–13]. However, challenges in implementation remain. Inconsistency between software packages and processing algorithms could result in increased variability of results. Greater image slice thickness and partial volume averaging have also been found to result in greater variability. Accurate nodule segmentation is of paramount importance; assessment could be compromised by inclusion of a peripheral or intervening pulmonary vessel or the adjacent pleura. Nodule density also poses a

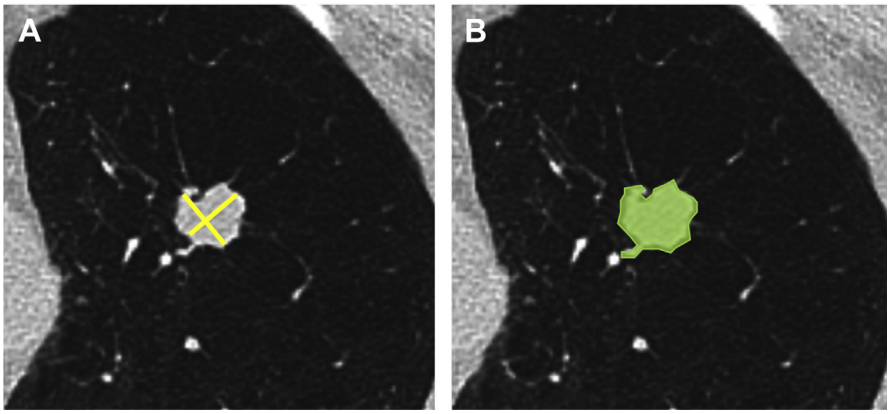

FIG. 1 Two methods of lung nodule measurement: (**A**) bidimensional linear measurements are averaged to provide nodule size (*calipers*); (**B**) semiautomated segmentation of the nodule (*green*) can be performed to more accurately determine nodule volume.

challenge, particularly in instances when a ground-glass attenuation nodule has a poorly marginated border [3].

Assessment of nodule mass, the product of volume and density, provides another indicator of change. However, in comparison to linear or volumetric nodule measurements, nodule mass provides an indication of growth that may be most applicable to subsolid lung nodules, which may change in nodule density or nodule volume over time. Investigation by de Hoop and colleagues [14] compared manual measurements of nodule diameter, volume, and mass of nonsolid ground-glass lung nodules in an effort to determine which measurement method was best to identify change. More than 120 data sets were used, involving more than 50 ground-glass nodules (GGN) identified on lung cancer screening studies, which were measured using electronic calipers and manually outlined to determine nodule volume and mass. The group found the smallest intraobserver and interobserver variability for GGN mass ($P<.001$), indicating that measurement of nodule mass can allow detection of GGN growth earlier and with less variability than diameter or volume measurements. In the setting of pulmonary adenocarcinoma lesions, increasing solid nodule density has been shown to correlate with invasive histopathology and staging, illustrating the relevance and potential value of lung nodule mass measurement [15–17].

UNDERSTANDING RADIOMICS

Quantitative CT imaging often finds itself under the conceptual heading of "radiomics." Radiomics refers to the extraction of numerous quantitative features from a region of interest (ROI), generating a large data set that can be used to numerically describe imaging features by hundreds of parameters [18]. These parameters can then be studied to determine patterns and relationships between imaging features and clinical information, which can in turn lead to discovery of novel imaging biomarkers and improved predictive capabilities, ultimately resulting in increased diagnostic accuracy.

Radiologic imaging relies on 2-dimensional or 3-dimensional (3D) data in the form of pixels or voxels, respectively. Regarding 3D CT data, quantitative values within these voxels can be used to generate an image. Four major technical categories of radiomics can be considered, in increasing complexity: these are intensity-based metrics, texture-based metrics, shape-based metrics, and finally, transform-based metrics [18]. Current clinical advancements have been made within the intensity-based and texture-based imaging realms.

Considering Histogram Features

Intensity-based imaging metrics use "first-order" statistics, specifically using data extracted from voxel values within an ROI. First-order statistics focus on the data within the voxel and do not consider spatial relationships between voxels. Voxel attenuation values obtained from within an ROI are typically distributed in the form of a histogram. The histogram illustrates the number of voxels (y-axis) distributed over a range of attenuation values (x-axis) (Fig. 2). The range of x-axis voxel attenuation values is often considered in terms of percentile ranges (such as 10% or 25% increments)

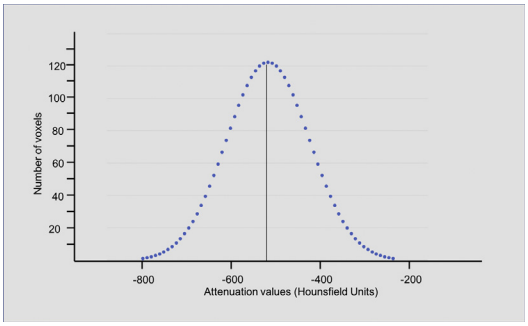

FIG. 2 Histogram with a normal distribution curve. Mean, median, and mode values are the same, indicated by straight black line. When used to assess subsolid lung nodules, for instance, the x-axis typically represents voxel attenuation value, whereas the y-axis typically represents the number of voxels.

or quartile ranges (first, second, third, or fourth quartile).

The diversity and distribution of data points on the histogram provide valuable information. When considering the shape of the histogram curve, it is best to remember a normal Gaussian distribution visualized as a symmetric bell curve: the mean (average of all data points), the median (the middle value of all data points), and the mode (the most frequent of all data points) are the same value, seen at the peak of the curve (see Fig. 2). In a normal distribution of data points, 1 standard deviation includes up to 68% of data points centered on the mean value. Two standard deviations from the mean value include up to 95% of data points, whereas 3 standard deviations encompass up to 99%. This characterization of data in relation to the mean can be very practical; 2 descriptors that are often used in the quantitative CT assessment of lung nodules are skewness and kurtosis.

The concept of skewness refers to asymmetric distribution of data points around the mean (Fig. 3) [19]. If data points are skewed to the left, the tail of the data curve is pulled to the left, and as a result, the mean value of the data comprising the curve is pulled to the left; leftward skewness is characterized as negative. This may be confusing visually, because the curve appears to be leaning to the right. Conversely, positive skewness refers to asymmetry of data points to the right; the tail of the curve is longer on the right, and the mean value of data points on the curve moves to the right. The curve may appear as though it is leftward leaning when, in fact, the right tail is elongated.

Kurtosis indicates how data points are distributed around the mean and is primarily a description of the tails of the distribution curve, rather than the peak of the curve (as was historically emphasized) (Fig. 4). A normal distribution curve has a kurtosis value of 3, but this is frequently manipulated mathematically such that a normal reference value is zero. Therefore, a distribution curve with positive kurtosis is described as having a steeper, narrower peak and, more importantly, heavier tails, with a larger number of data points falling outside 1 standard deviation. Conversely, a negative kurtosis would demonstrate a flatter curve and, more importantly, lighter tails, with fewer data points outside 1 standard deviation [20].

One important feature of histogram analysis is the diversity of data points that comprises the distribution, apart from the distribution of data points around the mean value. A heterogeneous sample of data points is thought to possess greater energy than a more uniform collection of data. A series of uniform data points reflects a series of predictable or highly probable events, which therefore provides less useful information. Conversely, one may consider an unpredictable or unlikely event, a random value within a heterogeneous set of data points, to hold more useful information. This concept of uncertainty or unpredictability conveys a higher potential for meaningful information [18]. The concept of entropy speaks to the diversity of information contained within the data set, and it can be referred to in the unit of a "bit." Regarding the histogram analysis, therefore, a lower entropy data set would be composed of more uniform data points, whereas a higher entropy data set would be more heterogeneous (Fig. 5).

Texture-based metrics are based on the concept of patterns: the repetitive nature of physical characteristics, such as shape, color, or intensity. Texture analysis, therefore, refers to the spatial relationships between voxel values rather than the data within the single voxel. Also referred to as "second-order" statistics, texture analysis attempts to answer questions such as how frequently similar voxel values are located near each other, in which direction and how far away, and what statistics can be derived from this information. Simply put, second-order statistics could be thought of as a matrix of voxel values; spatial relationships between voxel values extend a particular direction and distance, creating a textured pattern. This texture analysis, even more than first-order statistics, is thought to be applicable when assessing tumor heterogeneity [18]. Beyond texture analysis, higher-order statistics examine the relationship between 3 or more voxels.

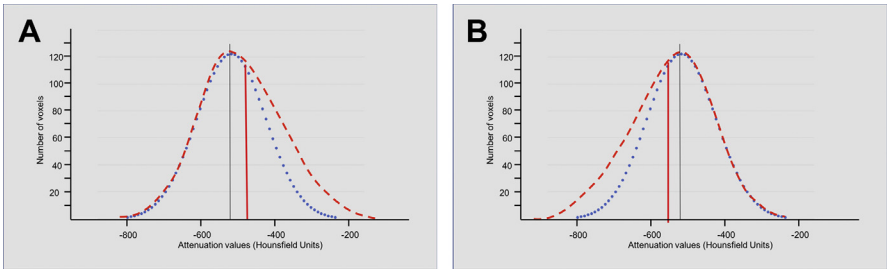

FIG. 3 Skewness. (**A**) Positive skewness indicates skewed data points to the right, resulting in an elongated right-sided tail of the distribution curve (*red dashed line*). The mean value also moves to the right (*solid red line*). (**B**) In contrast, negative skewness suggests distribution of data to the left of the expected mean, with elongation of the left-sided tail (*red dashed line*).

QUANTITATIVE COMPUTED TOMOGRAPHY AND LUNG NODULES: CLINICAL APPLICATIONS

As capabilities in data acquisition and processing have evolved, quantitative CT evaluation of lung nodules has captured the interest and imagination of researchers, particularly on the topic of subsolid lung nodules: nonsolid nodules composed of ground-glass attenuation with or without more solid attenuation components. After the reclassification of bronchoalveolar cell carcinoma into several more descriptive adenocarcinoma subtypes [16], there has been keen interest in determining what if any imaging characteristics could be used to differentiate lesions along this newly established pathologic spectrum. Initial radiologic descriptions of these entities focused on the visual determination of solid density: for example, adenocarcinoma in situ (AIS) was considered nonsolid on CT, whereas minimally invasive adenocarcinoma (MIA) was thought to be mainly nonsolid but could demonstrate a solid density component on CT up to roughly 5 mm [21]. Expected imaging appearances of lepidic predominant adenocarcinoma (LPA) and invasive mucinous adenocarcinoma were also described, as were other forms of invasive adenocarcinoma, differentiated by their predominant histopathologic features (acinar, papillary, or micropapillary, for example). As literature emerged describing qualitative imaging capabilities and imaging features of these entities (as illustrated in Figs. 6 and 7), differentiation of these subtypes became increasingly important as differences in 5-year survival rates became apparent. Although patients with AIS and MIA could expect a 5-year-survival rate of near 100%, more invasive adenocarcinoma subtypes, such as papillary, acinar, and micropapillary predominant lesions, saw declining 5-year survival rates of 71%, 68%, and 38%, respectively. The goal of many researchers, therefore, is the successful employment of quantitative CT to achieve radiologic subtyping of adenocarcinoma spectrum lesions. This subtyping could provide improved, more accurate prognostication, and it

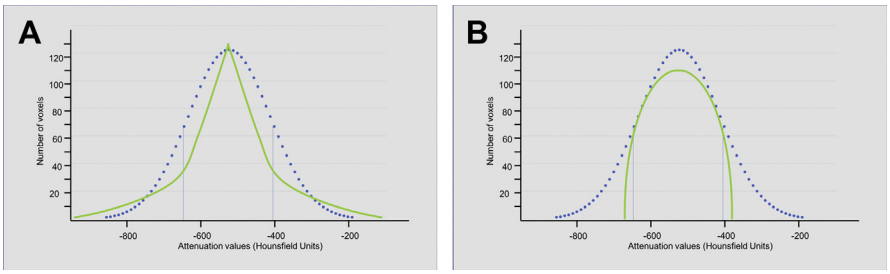

FIG. 4 Kurtosis. (**A**) Positive kurtosis indicates a relatively "heavy tail" with a larger number of data points outside of 1 standard deviation. The peak of the curve (*solid green line*) tends to be steeper and narrower. Thin blue lines indicate 1 standard deviation. (**B**) In contrast, negative kurtosis implies a "light tail," with most data points falling within 1 standard deviation and few outliers. Negative kurtosis may lead to a flatter distribution peak (*solid green line*).

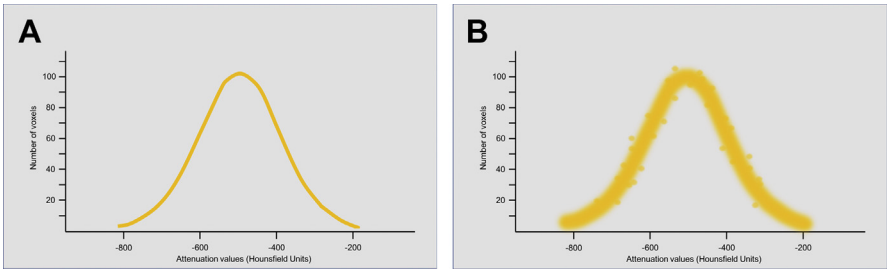

FIG. 5 Entropy indicates the heterogeneity of data points comprising the distribution curve. (**A**) A more uniform collection of data points can be compared with (**B**) a higher entropy collection of data, resulting in a less well-defined distribution curve.

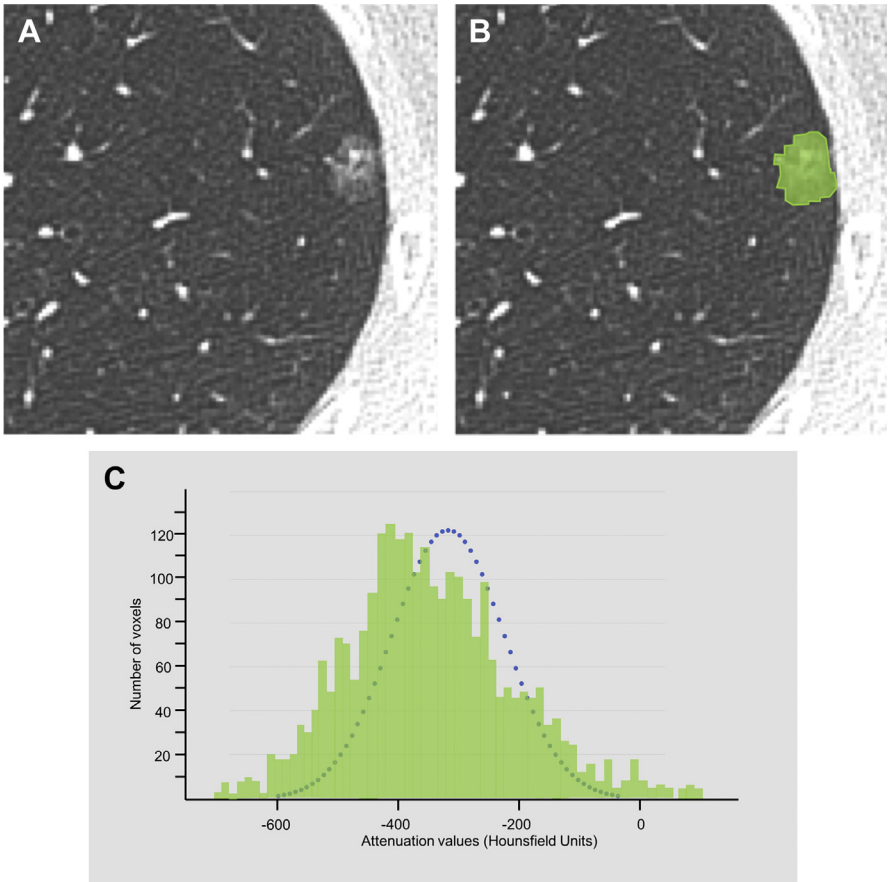

FIG. 6 (**A**) Pathologically proven MIA, up to 1.2 cm in diameter in the left upper lobe, demonstrating both ground-glass and solid attenuation. (**B**) Quantitative CT evaluation incorporates the use of an overlying voxel mask (shown in green). (**C**) The resultant histogram reflects the number of voxels with attenuation values in Hounsfield Units. This histogram is positively skewed to the right (s = 0.850), and the distribution demonstrates positive kurtosis (k = 2.938) with relatively heavy tails. A heterogeneous set of data points comprises the histogram, reflecting the entropy of the distribution curve (e = 5.986). For reference, the blue dotted line represents a normal distribution curve.

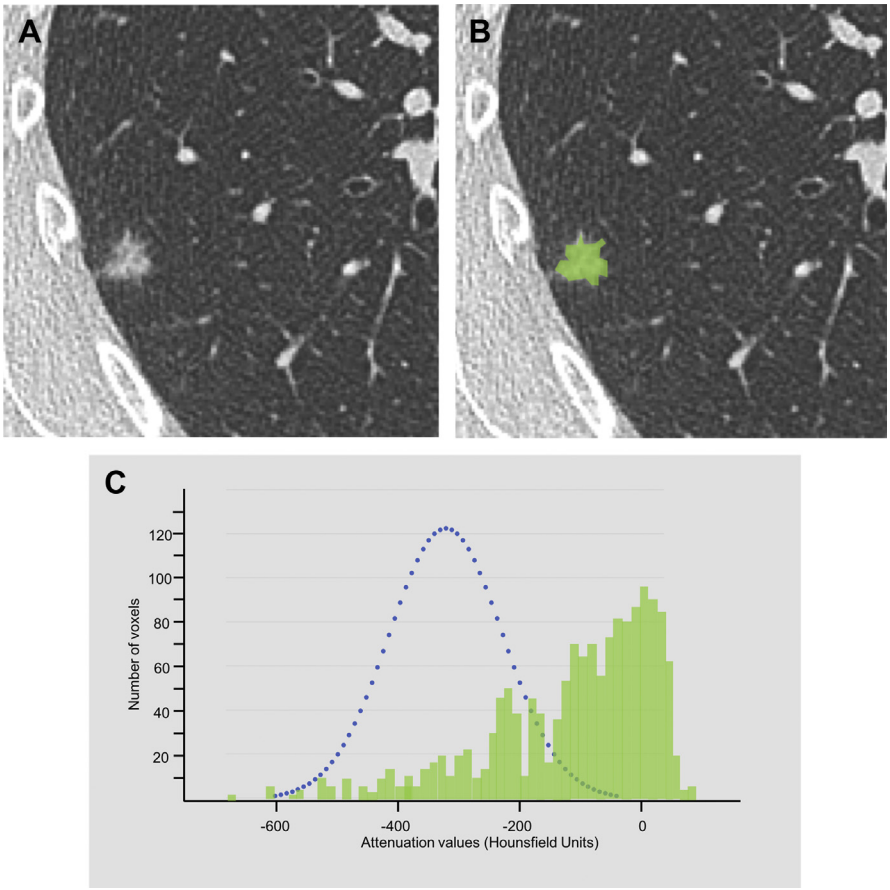

FIG. 7 (**A**) Pathologically proven invasive adenocarcinoma, up to 1.1 cm in the right upper lobe, demonstrating part-solid attenuation. (**B**) As shown, a voxel mask (shown in green) is placed over each thin-section axial image containing the nodule. (**C**) Resulting histogram demonstrates negative skewness, with data points skewed to the left (s = −2.352). Although overall kurtosis is 0.419, the right-sided tail of the distribution curve is light when compared with the left. For reference, the blue dotted line represents a normal distribution curve.

could potentially influence patient management in regards to the timing and necessity of surgical excision.

Investigating a group of 46 resected GGNs larger or equal to 10 mm, Lim and colleagues [22] studied both morphologic and quantitative imaging features and determined that nodule size (16.4 mm) and nodule mass (0.472 g) were significant features differentiating invasive adenocarcinoma from MIA or AIS lesions. Han and colleagues [23] later investigated a larger group of 163 GGNs in an attempt to distinguish a combined group of preinvasive and MIA from more invasive adenocarcinoma subtypes. Studying nodule diameter, area, volume, mass, and mean nodule attenuation, significant differences were found between the 2 groups among all measures. Using logistic regression analysis, the group reported that a cross-sectional area of 2.22 cm^2 was an independent predictor of invasive disease. Investigating the predictive value of solid volume within a lung nodule, Ko and colleagues [24] studied a group of subsolid lung nodules, a group that included both purely ground-glass and part-solid density nodules, and found statistically significant differences in mean percentage of solid volume between invasive adenocarcinoma (35.4%) and LPA (14.5%, $P = .002$). The group also found a near-significant trend between invasive adenocarcinoma and a combined group of AIS and MIA lesions, a result likely influenced by sample size (8.2%, $P = .051$).

In a later study, Li and colleagues [25] used quantitative assessment to differentiate preinvasive adenocarcinoma spectrum lesions from MIA and from more invasive adenocarcinoma subtypes. Investigating a group of 110 purely GGNs, the group found significant differences in nodule diameter, area, and mass between preinvasive and more invasive groups, although no significant difference could be documented between preinvasive and MIA lesions. However, it should be noted that when these 3 groups were assessed with more advanced histogram analysis, significant differences were found between CT attenuation percentiles of all 3 groups of nodules ($P<.05$). Additional study by Alpert and colleagues [26] also used both nodule volume and first-order statistical analysis to differentiate lesions on the adenocarcinoma spectrum. Citing improved 5-year survival among AIS, MIA, and LPA lesion patients, this study compared a combined group of lepidic predominant lesions with more invasive adenocarcinoma subtypes and found statistically significant differences between the 2 groups regarding nodule volume, percentage of solid volume, as well as first-order statistical histogram features, such as skewness, kurtosis, entropy, and mean nodule attenuation value within each histogram quartile.

Several other studies have attempted to demonstrate significant quantitative differences between invasive adenocarcinoma and groups of minimally and/or preinvasive lesions. Focusing on first-order statistical histogram features, Son and colleagues [27] studied nearly 200 GGNs, proven to represent invasive adenocarcinoma (n = 92), MIA (n = 61), and AIS (n = 38). Significant differences among these histopathologic groups of GGNs were discovered using histogram measures, such as 75% CT attenuation value (or third-quartile histogram values) and entropy (both $P<.05$). The following year, Hwang and colleagues [28] also found entropy to be a significant feature differentiating invasive adenocarcinoma lesions from MIA or preinvasive lesions, albeit with a smaller group of 66 purely GGNs. In distinction, Chae and colleagues [29] studied 86 part-solid nodules using multivariate analysis and reported smaller mass and higher kurtosis were significant features differentiating preinvasive lesions (atypical adenomatous hyperplasia and AIS) from invasive adenocarcinomas. Notably, this group also reported creation of an artificial neural network, which showed excellent accuracy differentiating preinvasive and invasive adenocarcinoma lesions using quantitative features of mean attenuation, mass, kurtosis, and entropy, with an area under curve = 0.981.

Future investigation focuses on quantitative CT characterization and subtyping of the various histopathologic subtypes of invasive adenocarcinoma, namely papillary, acinar, and micropapillary predominant pathologic conditions. A growing body of literature investigating the feasibility of second-order texture analysis of subsolid adenocarcinoma spectrum lesions is also anticipated.

CURRENT CHALLENGES

Despite radiologists' and scientists' interest in quantitative imaging, one of the greatest challenges remains the standardization of descriptive terms and imaging methods. One action to improve consistency across this growing body of literature is the creation of the Quantitative Imaging Biomarkers Alliance (QIBA), sponsored by the Radiological Society of North America. QIBA is a multidisciplinary consortium with the goal of enabling implementation and advancement of quantitative imaging methods. QIBA-published documents outline ways to reliably measure imaging features within a specific clinical context, while considering technical standards, how users interact and process data, and how users determine clinically meaningful metrics [30,31]. For example, a QIBA profile can outline a systematic approach to quantitative imaging to assess lung cancer screening–detected nodules [31]. In another example, varying data-processing algorithms could be applied to a reference data set of phantom lung nodules, and results could be used to determine reproducibility in accordance with a QIBA quantitative imaging profile [32]. In general, this process is designed to foster precise, reproducible ways to use quantitative imaging with the understanding that this evolving imaging approach will be implemented more and more into clinical care. As quantitative imaging gains greater clinical relevance, qualities such as reproducibility, cost, and improved patient outcomes all become paramount in importance.

Regarding lung nodules, the greatest disparity among quantitative CT literature is how study groups are defined by their pathologic diagnosis along the lung adenocarcinoma spectrum. For instance, some researchers investigate "preinvasive" lesions, including both atypical adenomatous hyperplasia and AIS lesions, whereas many others consider AIS alone. This preinvasive group may be compared directly with MIA lesions but is more commonly compared with "more invasive" adenocarcinoma subtypes (which may or may not include MIA). Many studies group preinvasive (AIS) and MIA lesions together, presumably because of

their similar near-100% 5-year survival rates, and then compare this group with a cohort of more frankly invasive adenocarcinoma lesions. At least 1 article advocates grouping all lepidic predominant lesions together (AIS, MIA, and LPA), a determination also based on the similarly high 5-year survival rate for all 3 pathologic diagnoses [26]. Another potential source of inconsistency among literature is the investigation of lung nodules based on a more qualitative assessment of visual attenuation. Specifically, many studies only include purely ground-glass attenuation nodules. Studies that include part-solid density nodules as part of a study cohort typically approach that population with a known pathologic diagnosis rather than a qualitative density assessment. Subtle disparities in study design such as these may make it more challenging to apply conclusive findings to everyday clinical practice.

Apart from inconsistencies in study design, the major hurdle that remains in the clinical realm is implementation of quantitative CT imaging in the reading room, enabling radiologists to include this assessment in their daily workflow. As the body of literature expands, and quantitative CT finds greater validation and acceptance, the need for this evolving imaging technology will continue to grow. Accessibility of automated software to extract and process data poses a challenge, although the development of automated nodule selection tools would greatly influence the time and work required to incorporate this technology into clinical workflow. Ideally, quantitative CT technique and processing have to be implemented in a facile way that can efficiently and seamlessly be incorporated into the radiologists' already busy and complex workday.

SUMMARY

Although the clinical expertise of an experienced radiologist will always be needed, quantitative assessment of indeterminate lung nodules provides objective data pertaining to nodule size, volume, density, and mass. Lung nodule volumetry has been shown to provide a more accurate determination of nodule size than simple caliper measurements. Further still, significant advancements in CT imaging technology and data-processing software now allow evaluation of data at the level of the 3D voxel, exposing a wealth of data that has been traditionally underutilized. The application of first-order statistical analysis of voxel attenuation, specifically attenuation data of subsolid lung nodules that may lie along a spectrum of adenocarcinoma subtypes, has led to the publication of a robust and growing body of literature. Although challenges exist, there has been progress in radiologic subtyping of adenocarcinoma spectrum lesions, with most straightforward quantitative differences demonstrated between preinvasive and minimally invasive adenocarcinoma and more invasive subtypes. As technical capabilities improve, additional in-depth investigation of indeterminate lung nodules with first-order histogram and second-order texture analysis techniques are sure to follow.

REFERENCES

[1] Erasmus JJ, Gladish GW, Broemeling L, et al. Interobserver and intraobserver variability in measurement of non-small-cell carcinoma lung lesions: implications for assessment of tumor response. J Clin Oncol 2003;21(13):2574–82.

[2] Revel MP, Bissery A, Bienvenu M, et al. Are two-dimensional CT measurements of small noncalcified pulmonary nodules reliable? Radiology 2004;231(2):453–8.

[3] Devaraj A, van Ginneken B, Nair A, et al. Use of volumetry for lung nodule management: theory and practice. Radiology 2017;284(3):630–44.

[4] MacMahon H, Naidich DP, Goo JM, et al. Guidelines for management of incidental pulmonary nodules detected on CT images: from the Fleischner Society 2017. Radiology 2017;284(1):228–43.

[5] Horeweg N, van Rosmalen J, Heuvelmans MA, et al. Lung cancer probability in patients with CT-detected pulmonary nodules: a prespecified analysis of data from the NELSON trial of low-dose CT screening. Lancet Oncol 2014;15(12):1332–41.

[6] van Klaveren RJ, Oudkerk M, Prokop M, et al. Management of lung nodules detected by volume CT scanning. N Engl J Med 2009;361(23):2221–9.

[7] Gould MK, Donington J, Lynch WR, et al. Evaluation of individuals with pulmonary nodules: when is it lung cancer? Diagnosis and management of lung cancer, 3rd ed: American College of Chest Physicians evidence-based clinical practice guidelines. Chest 2013;143(5 Suppl):e93S–120S.

[8] Gould MK, Fletcher J, Iannettoni MD, et al. Evaluation of patients with pulmonary nodules: when is it lung cancer?: ACCP evidence-based clinical practice guidelines (2nd edition). Chest 2007;132(3 Suppl):108S–30S.

[9] Heuvelmans MA, Oudkerk M, de Bock GH, et al. Optimisation of volume-doubling time cutoff for fast-growing lung nodules in CT lung cancer screening reduces false-positive referrals. Eur Radiol 2013;23(7):1836–45.

[10] Mehta HJ, Ravenel JG, Shaftman SR, et al. The utility of nodule volume in the context of malignancy prediction for small pulmonary nodules. Chest 2014;145(3):464–72.

[11] Goodman LR, Gulsun M, Washington L, et al. Inherent variability of CT lung nodule measurements in vivo using semiautomated volumetric measurements. AJR Am J Roentgenol 2006;186(4):989–94.
[12] Bogot NR, Kazerooni EA, Kelly AM, et al. Interobserver and intraobserver variability in the assessment of pulmonary nodule size on CT using film and computer display methods. Acad Radiol 2005;12(8):948–56.
[13] Wormanns D, Kohl G, Klotz E, et al. Volumetric measurements of pulmonary nodules at multi-row detector CT: in vivo reproducibility. Eur Radiol 2004;14(1):86–92.
[14] de Hoop B, Gietema H, van de Vorst S, et al. Pulmonary ground-glass nodules: increase in mass as an early indicator of growth. Radiology 2010;255(1):199–206.
[15] Ko JP, Azour L. Management of incidental lung nodules. Semin Ultrasound CT MR 2018;39(3):249–59.
[16] Travis WD, Asamura H, Bankier AA, et al. The IASLC lung cancer staging project: proposals for coding T categories for subsolid nodules and assessment of tumor size in part-solid tumors in the forthcoming eighth edition of the TNM classification of lung cancer. J Thorac Oncol 2016;11(8):1204–23.
[17] Cho JY, Leem CS, Kim Y, et al. Solid part size is an important predictor of nodal metastasis in lung cancer with a subsolid tumor. BMC Pulm Med 2018;18(1):151.
[18] Kolossvary M, Kellermayer M, Merkely B, et al. Cardiac computed tomography radiomics: a comprehensive review on radiomic techniques. J Thorac Imaging 2018;33(1):26–34.
[19] Doane DP, Seward LE. Measuring skewness: a forgotten statistic? J Stat Educ 2011;19(2):18.
[20] DeCarlo LT. On the meaning and use of kurtosis. Psychol Methods 1997;2:292–307.
[21] Austin JH, Garg K, Aberle D, et al. Radiologic implications of the 2011 classification of adenocarcinoma of the lung. Radiology 2013;266(1):62–71.
[22] Lim HJ, Ahn S, Lee KS, et al. Persistent pure ground-glass opacity lung nodules $\geq$ 10 mm in diameter at CT scan: histopathologic comparisons and prognostic implications. Chest 2013;144(4):1291–9.
[23] Han L, Zhang P, Wang Y, et al. CT quantitative parameters to predict the invasiveness of lung pure ground-glass nodules (pGGNs). Clin Radiol 2018;73(5):504.e1–7.
[24] Ko JP, Suh J, Ibidapo O, et al. Lung adenocarcinoma: correlation of quantitative CT findings with pathologic findings. Radiology 2016;280(3):931–9.
[25] Li Q, Fan L, Cao ET, et al. Quantitative CT analysis of pulmonary pure ground-glass nodule predicts histological invasiveness. Eur J Radiol 2017;89:67–71.
[26] Alpert JB, Rusinek H, Ko JP, et al. Lepidic predominant pulmonary lesions (LPL): CT-based distinction from more invasive adenocarcinomas using 3D volumetric density and first-order CT texture analysis. Acad Radiol 2017;24(12):1604–11.
[27] Son JY, Lee HY, Lee KS, et al. Quantitative CT analysis of pulmonary ground-glass opacity nodules for the distinction of invasive adenocarcinoma from pre-invasive or minimally invasive adenocarcinoma. PLoS One 2014;9(8):e104066.
[28] Hwang IP, Park CM, Park SJ, et al. Persistent pure ground-glass nodules larger than 5 mm: differentiation of invasive pulmonary adenocarcinomas from preinvasive lesions or minimally invasive adenocarcinomas using texture analysis. Invest Radiol 2015;50(11):798–804.
[29] Chae HD, Park CM, Park SJ, et al. Computerized texture analysis of persistent part-solid ground-glass nodules: differentiation of preinvasive lesions from invasive pulmonary adenocarcinomas. Radiology 2014;273(1):285–93.
[30] Kessler LG, Barnhart HX, Buckler AJ, et al. The emerging science of quantitative imaging biomarkers terminology and definitions for scientific studies and regulatory submissions. Stat Methods Med Res 2015;24(1):9–26.
[31] Mulshine JL, Gierada DS, Armato SG 3rd, et al. Role of the quantitative imaging biomarker alliance in optimizing CT for the evaluation of lung cancer screen-detected nodules. J Am Coll Radiol 2015;12(4):390–5.
[32] Athelogou M, Kim HJ, Dima A, et al. Algorithm variability in the estimation of lung nodule volume from phantom CT scans: results of the QIBA 3A public challenge. Acad Radiol 2016;23(8):940–52.